

## Thermoelectric properties of some metal borides

Masatoshi Takeda,\* Tadahiro Fukuda, Ferrer Domingo, and Takahiro Miura

*Department of Mechanical Engineering, Nagaoka University of Technology, 1603-1 Kamitomioka, Nagaoka 940-2188, Japan*

Received 1 October 2002; accepted 27 February 2003

### Abstract

Polycrystalline  $\text{AlMgB}_{14}$  and some hexaborides ( $\text{CaB}_6$ ,  $\text{SrB}_6$ ,  $\text{YbB}_6$ ,  $\text{SmB}_6$ , and  $\text{CeB}_6$ ) were synthesized to examine their thermoelectric properties. Single phase of orthorhombic  $\text{AlMgB}_{14}$ , which contains  $\text{B}_{12}$  icosahedral clusters as building blocks, was obtained at sintering temperatures between 1573 and 1823 K. Seebeck coefficient ( $\alpha$ ) and electrical conductivity ( $\sigma$ ) of the phase were about  $500 \mu\text{V/K}$  and  $10^{-1} \text{I}/\Omega\text{m}$  at room temperature, respectively. These values are comparable to those of metal-doped  $\beta$ -rhombohedral boron. On the other hand, metal hexaborides with divalent cation possessed large negative  $\alpha$  ranging from  $-100$  to  $-270 \mu\text{V/K}$  at 1073 K. Calculated power factors of  $\text{CaB}_6$  and  $\text{SrB}_6$  exceeded  $10^{-3} \text{W/K}^2\text{m}$  within the entire range of temperature measured. As a result, they can be thought as promising candidates for  $n$ -type thermoelectric material.

© 2003 Elsevier Inc. All rights reserved.

**Keywords:**  $\text{AlMgB}_{14}$ ; Hexaboride; Seebeck coefficient; Electrical conductivity; Power factor

### 1. Introduction

One of the promising application fields for boron-rich solids is high-temperature thermoelectric (TE) conversion [1]. Intensive studies on TE properties have been carried out on boron carbides [2] including single crystals [3] and thin films [4], and metal-doped  $\beta$ -rhombohedral boron ( $\beta$ -boron) [5,6] because of their large Seebeck coefficient ( $\alpha$ ) and low thermal conductivity. They contain 12-atom icosahedral clusters ( $\text{B}_{12}$ ) as building blocks, and their large  $\alpha$  and hopping type conduction are attributed to the existence of the clusters [7]. At high temperatures, the boron carbides'  $\alpha$  is temperature independent or slightly increases with temperature, while the electrical conductivity ( $\sigma$ ) increases [3]. As a consequence, relatively large TE figure-of-merit,  $Z$ , can be obtained at high temperatures. However, all boron carbides and doped ones [8–11] studied are  $p$ -type semiconductor except for  $n$ -type behavior reported in Ni-doped ones [12,13]. As for the  $\beta$ -boron, metal-doped ones have been studied to improve TE properties and to search for  $n$ -type materials. Significant increase in  $\sigma$  by the doping results in the improvement of total performance, although the

absolute value of the  $\alpha$  decreases. The doping of certain metals, such as V, Cr and Fe, changes  $\alpha$  from positive to negative [5,6,14], but the TE properties of the  $n$ -type boron-rich semiconductors were insufficient compared to  $p$ -type ones. Whereas further doping will be effective for improvement, it is difficult to increase doping level, because maximum amount of dopant is limited to a few percent due to the restriction of the doping site in the crystal structure. It is, therefore, of practical and scientific interest to investigate TE properties of borides other than boron carbide or  $\beta$ -boron type structure, which have higher metal-to-boron ratio.

In the present study, we synthesized and examined some metal borides, more specifically,  $\text{AlMgB}_{14}$  and metal hexaborides ( $\text{CaB}_6$ ,  $\text{SrB}_6$ ,  $\text{YbB}_6$ ,  $\text{SmB}_6$ , and  $\text{CeB}_6$ ). The  $\text{AlMgB}_{14}$  is an orthorhombic phase containing  $\text{B}_{12}$  icosahedral clusters identical with those in  $\beta$ -boron, but arrangement of the cluster is different. In the  $\text{AlMgB}_{14}$  structure, there are large openings that can accommodate boron, aluminum, or magnesium atoms. The hexaborides have almost the same metal-to-boron ratio as  $\text{AlMgB}_{14}$  phase, but the clusters constituting the hexaboride are octahedrons. They possess semiconducting or metallic character in accordance with the constituent metal [15]. We examined TE properties of these metal borides, and discussed their potential as TE materials.

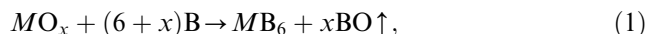
\*Corresponding author. Fax: +81-258-47-9770.

E-mail address: [takeda@mech.nagaokaut.ac.jp](mailto:takeda@mech.nagaokaut.ac.jp) (M. Takeda).

## 2. Experimental

Polycrystalline bulk of  $\text{AlMgB}_{14}$  was prepared by pulsed electric current sintering (PECS) method. Prior to the sintering, precursor powders of Al–B and Mg–B with a metal/boron ratio of 1/7 were prepared because melting temperatures of Al and Mg are extremely low compared to that of boron. For the preparation of the precursors, Al (99.99% purity), Mg (99.9% purity), and B (99% purity) powders were used. Mixture of the precursors was then sintered at 50 MPa for 15 min under Ar (99.99% purity) atmosphere.

We prepared powders of hexaborides according to the borothermal reaction,



where  $M$  is Ca, Sr, Yb, Sm, or Ce. A mixture of metal-oxide and B powders was pressed into a pellet, and heated at 1473 K for 24 h in vacuum. The metal-oxides used as starting materials were  $\text{CaO}$  (99.9% purity),  $\text{SrO}$  (99% purity),  $\text{Yb}_2\text{O}_3$  (99.99% purity),  $\text{Sm}_2\text{O}_3$  (99.9% purity), and  $\text{CeO}_2$  (99.99% purity). The resultant  $\text{MB}_6$  powders were then sintered by the PECS at 2073 K and 50 MPa under Ar atmosphere.

The phases of the powders and the sintered bodies were determined by XRD, and microstructure of the bulks was observed by SEM. Electron probe micro analysis (EPMA) was used to examine contamination and segregation in the sintered specimens. Only the constituent elements were detected by the EPMA, but it was difficult to determine precisely the composition of the specimens, because of the low sensitivity of the EPMA to light elements such as B. In the present paper, we use the nominal compositions of the specimens.

The  $\sigma$  of the specimens cut into rectangular plates was measured by standard four-probe technique. The  $\alpha$  of them was calculated from the slope of several thermoelectric voltage vs. temperature difference measurements and corrected for the probe leads. These thermoelectric properties were measured from room temperature up to 1073 K.

## 3. Results and discussion

### 3.1. $\text{AlMgB}_{14}$

XRD measurements revealed that single phase of orthorhombic  $\text{AlMgB}_{14}$  phase was obtained at sintering temperatures between 1573 and 1823 K, while higher sintering temperatures led to the appearance of  $\gamma$ - $\text{AlB}_{12}$ -type phase. Temperature dependence of the TE properties was measured for the  $\text{AlMgB}_{14}$  sintered at 1773 K. Temperature dependence of the  $\sigma$  and the  $\alpha$  are shown in Figs. 1 and 2, respectively, together with corresponding data for a boron carbide,  $\beta$ -boron, and Mg-doped  $\beta$ -

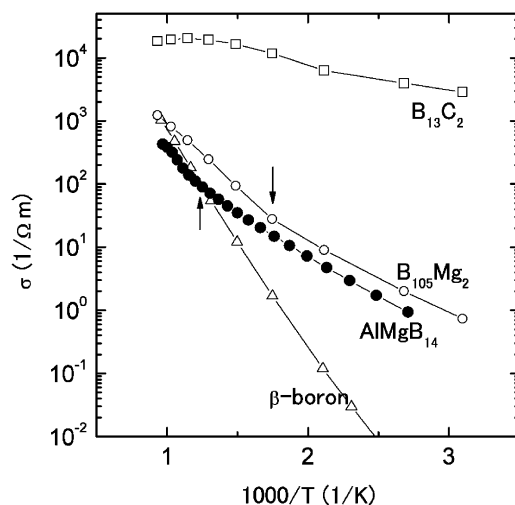


Fig. 1. Temperature dependence of electrical conductivity of sintered  $\text{AlMgB}_{14}$ . For comparison, those of boron carbide,  $\beta$ -boron, and  $\text{Mg}_2\text{B}_{105}$  are also shown. The arrows indicate the small kink (see text).

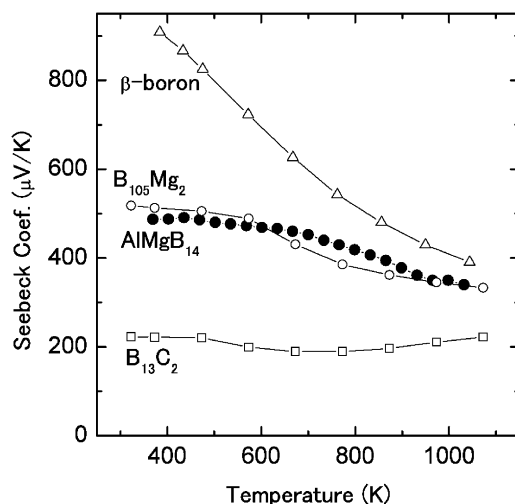


Fig. 2. Temperature dependence of Seebeck coefficient of sintered  $\text{AlMgB}_{14}$ . For comparison, those of boron carbide,  $\beta$ -boron, and  $\text{Mg}_2\text{B}_{105}$  are also shown.

boron ( $\text{B}_{105}\text{Mg}_2$ ), which were also synthesized by the same sintering method as that used for the  $\text{AlMgB}_{14}$  and the metal hexaborides. The  $\text{AlMgB}_{14}$ 's  $\sigma$  is comparable to that of  $\text{Mg}_2\text{B}_{105}$  and exhibits similar temperature dependence, in which there is a small kink. Temperature dependence of the  $\sigma$  for  $\text{AlMgB}_{14}$  and  $\text{Mg}_2\text{B}_{105}$  is likely to be explained by hopping-type conduction rather than Arrhenius-type conduction below the temperature at which the small kink appeared. Hopping-type conduction mechanisms are usually applied to explain transport property of boron-rich semiconductors [16,17]. Temperature dependence of boron carbides'  $\sigma$  can be explained by bipolaron hopping expressed as

$$\sigma T = A \exp(-E/kT), \quad (2)$$

while variable-range-hopping expressed as

$$\sigma = \sigma_0 \exp\{-(T_0/T)^{1/4}\} \quad (3)$$

is applied to explain those of metal-doped  $\beta$ -borons'  $\sigma$  in many cases. However, difference in temperature dependence among these two hopping conduction and Arrhenius-type conduction is small when temperature range is not wide enough. It is therefore difficult to determine conduction-type of  $\text{AlMgB}_{14}$  from the  $\sigma$ .

As shown in Fig. 2, the  $\alpha$  of the  $\text{AlMgB}_{14}$  is positive and large, which is similar to those of other boron-rich semiconductors containing icosahedral clusters. Almost temperature independent or slightly increasing temperature dependence of  $\alpha$  at high temperatures is predicted by theories on hopping conduction [16,18–20]; actually, boron carbide exhibits such temperature dependence. As for the  $\text{AlMgB}_{14}$ ,  $\alpha$  exhibits weak temperature dependence at lower temperature measured, while it decreases more rapidly at higher temperature. Such a situation is also observed in  $\text{Mg}_2\text{B}_{105}$ . It seems that the weak temperature dependence in  $\alpha$  is consistent with hopping-type behavior in  $\sigma$ . And the decrease in  $\alpha$  at high temperatures may be attributed to the increase of thermally activated carriers with temperature.

### 3.2. Hexaborides

According to EPMA analysis, there were B and  $\text{CaB}_6$  phases in the sintered  $\text{CaB}_6$  specimen, while no B peak could be observed by XRD. Since the amount of B phase is small, the measured thermoelectric properties are considered to represent those of  $\text{CaB}_6$  phase. As for the other hexaborides prepared, no secondary phase was detected by XRD, SEM, and EPMA. Relative density of the specimens was more than 90%, and there was no significant difference among the specimens studied.

Figs. 3 and 4 show temperature dependence of  $\sigma$  and  $\alpha$ , respectively. As shown in the figures, the divalent hexaborides ( $\text{CaB}_6$ ,  $\text{SrB}_6$ , and  $\text{YbB}_6$ ) possess large negative  $\alpha$  with relatively large  $\sigma$ , while the  $\alpha$  for trivalent hexaboride ( $\text{CeB}_6$ ) is small. The trivalent hexaborides are understood as metallic systems, and divalent ones are considered as semiconductors or semimetals [15,21,22]. The small  $\alpha$  and large  $\sigma$  of  $\text{CeB}_6$  are typical character of metals. The intermediate-valent hexaboride ( $\text{SmB}_6$ ) possess small  $\alpha$  above room temperature, although large negative  $\alpha$  was reported at low temperatures [23]. These results suggest that the trivalent and intermediate-valent hexaborides are not suitable for high-temperature TE material.

In the case of divalent hexaborides, early theoretical study predicted the divalent hexaborides to be polar semiconductors, with a complete charge transfer from metal atom to the  $\text{B}_6$  octahedron [24]. Recent band calculations, however, have shown that the changes in inter- and intra-octahedron B–B distances can easily

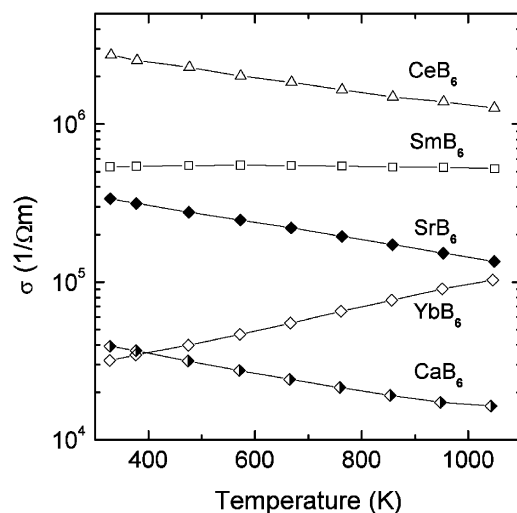


Fig. 3. Temperature dependence of electrical conductivities of hexaborides.

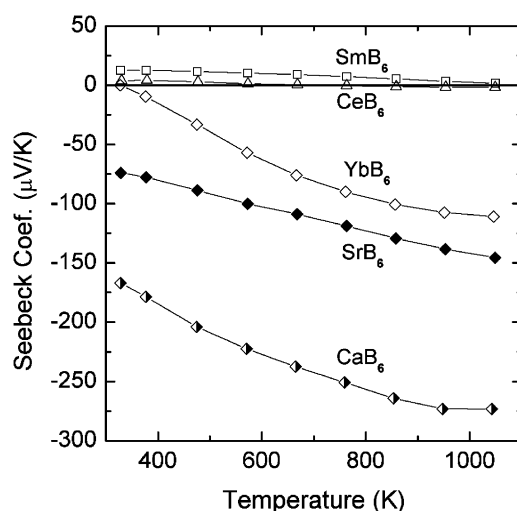


Fig. 4. Temperature dependence of Seebeck coefficients of hexaborides.

change the electronic property of the hexaborides from small gap semiconductor to semimetal, resulting from slight band overlapping [22,25]. The metallic temperature dependence of the  $\sigma$  observed in the divalent hexaborides except for  $\text{YbB}_6$  appears to be attributed to the band overlapping. And the large negative Seebeck coefficients indicate a low concentration of  $n$ -type carriers at the Fermi level. The different behavior between  $\text{YbB}_6$  and other divalent hexaborides may be caused by the compositional and structural difference, namely non-stoichiometry and structural defect, which affect the band overlapping of the divalent hexaborides. Further investigation is needed to elucidate the origin of the difference. Nevertheless, present results and previously reported theoretical and experimental results

suggest that the negative Seebeck coefficient is a common feature of the divalent hexaborides. Imai et al. predicted a negative Seebeck coefficient in divalent hexaborides on the basis of first principle calculations and Mott's theory [26], and negative  $\alpha$  was reported in  $\text{CaB}_6$ ,  $\text{YbB}_6$ , and  $\text{EuB}_6$  [27–30]. To the best of our knowledge, TE properties of  $\text{SrB}_6$  have never been reported. As shown in Fig. 4,  $\text{SrB}_6$  also possesses large negative  $\alpha$ .

### 3.3. Power factor

Fig. 5 shows the power factors (PF), expressed as  $\alpha^2\sigma$ , for  $\text{AlMgB}_{14}$  and divalent hexaborides together with those of the boron carbide and the  $\text{Mg}_2\text{B}_{105}$  for comparison. The  $\text{AlMgB}_{14}$ 's PF is comparable to that of the  $\text{Mg}_2\text{B}_{105}$  and increases with temperature. However, their low  $\sigma$ s lead to their PF insufficient for the TE application.

In contrast, the divalent hexaborides possess large PF values. Particularly, the PFs of  $\text{CaB}_6$  and  $\text{SrB}_6$  are larger than that of boron carbide in the entire range of temperature we measured, and their PF are almost temperature independent, which suggests the possibility to be used within a wide temperature range.

## 4. Conclusions

The  $\text{AlMgB}_{14}$  is a semiconductor with a large positive  $\alpha$ , which is similar to most of boron-rich semiconductors. However, its TE property was insufficient for practical applications due to its low  $\sigma$ .

The divalent hexaborides ( $\text{CaB}_6$ ,  $\text{SrB}_6$ , and  $\text{YbB}_6$ ) are *n*-type materials with relatively large  $\alpha$  and  $\sigma$ , whereas

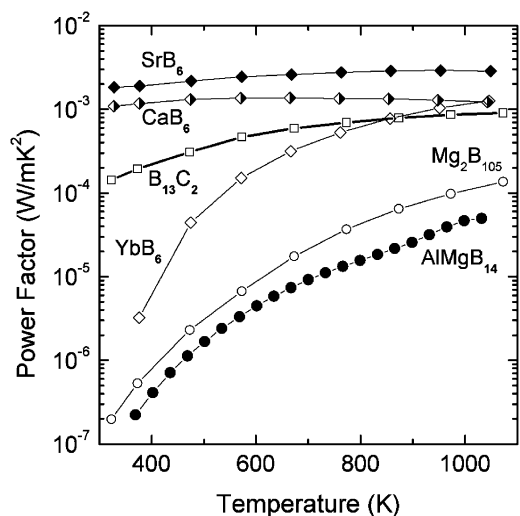


Fig. 5. Calculated power factors of  $\text{AlMgB}_{14}$  and divalent hexaborides. For comparison, those of boron carbide and  $\text{Mg}_2\text{B}_{105}$  are also shown.

trivalent and intermediate-valent ones possess  $\alpha$ s as small as those of typical metals. In particular,  $\text{CaB}_6$  and  $\text{SrB}_6$  were found to be promising candidates for *n*-type TE materials in boron-rich solids, because their PFs were larger than boron carbide and comparable to those of TE materials currently used. Measurements on thermal conductivity and further improvements are necessary for the TE application. The substitution of metal atoms in the hexaborides with other atoms might be effective to reduce the thermal conductivity and improve the electrical properties. Such attempts are now in progress.

## Acknowledgments

This work was supported in part by Yazaki Memorial Foundation for Science & Technology and by New Energy and Industrial Technology Development Organization (NEDO).

## References

- [1] C. Wood, Boron-rich solids, in: D. Emin, T.L. Aselage, C.L. Beckel, I.A. Howard, C. Wood (Eds.), AIP Conference Proceeding, Vol. 140, American Institute of Physics, New York, 1985, p. 362.
- [2] M. Bouchacourt, F. Thevenot, J. Mater. Sci. 20 (1985) 1237; H. Werheit, Mater. Sci. Eng. B 29 (1995) 228.
- [3] I. Gunjishima, T. Akashi, T. Goto, Mater. Trans. 42 (2001) 1445.
- [4] H. Suematsu, K. Kitajima, I. Ruiz, K. Kobayashi, M. Takeda, D. Shimbo, T. Suzuki, W. Jiang, K. Yatsui, Thin Solid Films 407 (2002) 132–135.
- [5] H. Werheit, R. Schmechel, V. Fueffel, T. Lundström, J. Alloys Compd. 262 (1997) 372.
- [6] T. Nakayama, J. Shimizu, K. Kimura, J. Solid State Chem. 154 (2000) 13.
- [7] T.L. Aselage, D. Emin, S.S. McCready, R.V. Duncan, Phys. Rev. Lett. 81 (1998) 2316.
- [8] T.L. Aselage, D. Emin, G.A. Samara, D.R. Tallant, S.B. Van Deusen, M.O. Eatough, H.L. Tardy, E.L. Venturini, Phys. Rev. B 48 (1993) 11759.
- [9] K.-f. Cai, C.-W. Nan, X.-M. Min, Mat. Res. Soc. Symp. Proc. 545 (1999) 131.
- [10] K.-f. Cai, C.-W. Nan, Y. Paderno, D.S. McLachlan, Solid State Commun. 115 (2000) 523.
- [11] C.H. Liu, Mater. Sci. Eng. B 72 (2000) 23.
- [12] S. Hwang, K. Yang, P.A. Dowben, A.A. Ahmad, N.J. Ianno, J.Z. Li, J.Y. Lin, H.X. Jiang, D.N. McIlroy, Appl. Phys. Lett. 77 (1997) 1028.
- [13] C.H. Liu, Mater. Lett. 49 (2001) 308.
- [14] U. Kuhlmann, H. Werheit, T. Dose, T. Lundström, J. Alloys Compd. 186 (1992) 187.
- [15] J. Etourneau, P. Hagenmuller, Philos. Mag. B 52 (1985) 589.
- [16] C. Wood, D. Emin, Phys. Rev. B 29 (1984) 4582.
- [17] H. Matsuda, T. Nakayama, K. Kimura, Y. Murakami, H. Suematsu, M. Kobayashi, I. Higashi, Phys. Rev. B 52 (1995) 6102.
- [18] T.L. Aselage, D. Emin, S.S. McCready, Phys. Rev. B 64 (2001) 54302.
- [19] W. Brenig, G.H. Döhler, P. Wölfe, Z. Phys. 258 (1973) 381.
- [20] H. Overhof, Phys. Stat. Solidi B 67 (1975) 709.

- [21] M. Aono, S. Kawai, S. Kono, M. Okusawa, T. Sagawa, Y. Takehana, *J. Phys. Chem. Solids* 37 (1976) 215.
- [22] S. Massidda, A. Continenza, T.M. de Pascale, R. Monnier, *Z. Phys. B* 102 (1997) 83.
- [23] N.E. Sluchanko, A.A. Volkov, V.V. Glushkov, B.P. Gorshunov, S.V. Demishev, M.V. Kondrin, A.A. Pronin, N.A. Samarin, Y. Bruynseraede, V.V. Moshchalkov, S. Kunii, *JETP* 88 (1999) 533.
- [24] H.C. Longuet-Higgins, M.V. de Robert, *Proc. Roy. Soc. Lond. A* 224 (1965) 336.
- [25] K. Schmitt, C. Stückl, H. Ripplinger, B. Albert, *Solid State Sci.* 3 (2001) 321.
- [26] Y. Imai, M. Mukaida, M. Ueda, A. Watanabe, *Intermetallics* 9 (2001) 721.
- [27] N. Takashima, J. Kawano, K. Mori, Y. Nishi, Y. Miyazawa, J. Matsushita, *Proceedings of the 44th International SAMPE Symposium, 1999*, pp. 2406.
- [28] K. Gianno, A.V. Sologubenko, H.R. Ott, A.D. Bianchi, Z. Fisk, *J. Phys.: Condens. Matter* 14 (2002) 1035.
- [29] J.M. Tarascon, J. Etourneau, P. Dordor, P. Hagenmuller, M. Kasaya, J.M.D. Coey, *J. Appl. Phys.* 51 (1980) 574.
- [30] V.A. Sidorov, N.N. Stepanov, O.B. Tsiok, L.G. Khvostantsev, I.A. Smirnov, M.M. Korsukova, *Sov. Phys. Solid State* 33 (1991) 720.